ORIGINAL

Effect of fatigue and annual rings' orientation on mechanical properties of wood under cross-grain uniaxial compression

A. Miksic · M. Myntti · J. Koivisto · L. Salminen · M. Alava

Abstract The mechanics of fresh wood with and without a fatigue pre-treatment that mimics a mechanical pulping process was experimentally studied. The mechanical properties of Norway spruce samples under compression are considered with the macroscopic stress–strain data and from local strain properties via digital image correlation technique. The results highlight the effects of the orientation of the wood annual rings compared to the loading direction and of the pre-fatigue. The wood presents a low yield point when the annual rings are tilted compared to the load axis, but the Young's modulus and yield stress are higher when the annual rings are either parallel or perpendicular to the load direction. In the last case, buckling of softest layers occurs. The fatigue treatment makes the wood less stiff as deduced from the decreases of Young's modulus and yield stress, whatever the orientation of annual rings. Secondly, it creates a thin and localized softened layer.

Introduction

Wood is a viscoelastic composite material (Findley et al. 1989; Schniewind and Barrett 1972) which has been studied since a long time in various cases: creep and relaxation (Ansell 2011; Navi and Stanzl-Tschegg 2009; Hanhijärvi and Hunt 1998; Armstrong and Kingston 1960), for the effect of moisture (Ozyhar et al. 2012;

A. Miksic (✉)
Istituto dei Sistemi Complessi - CNR, Via del Fosso del Cavaliere 100, 00133 Rome, Italy
e-mail: amandine.miksic@aalto.fi

A. Miksic · M. Myntti · J. Koivisto · M. Alava
Department of Applied Physics, COMP Center of Excellence, Aalto University School of Science,
P.O. Box 14100, 00076 Aalto, Finland

L. Salminen
VTT Technical Research Center of Finland, P.O. Box 1000, 02044 VTT, Finland

Ansell 2011; Wildehammar 2004; Hanhijärvi and Hunt 1998; Armstrong and Kingston 1960) or temperature (Kärenlampi et al. 2003; Uhmeier and Salmen 1996a), or in order to understand its properties at the scale of the wood cells (Ansell 2011; Jäger et al. 2011; Salmén and Burgert 2009; Keckes et al. 2003; Murata and Masuda 2001). Among various cases of practical importance, the slow fatigue of dry wood is interesting because wood is an important building material. Both the understanding of fatigue effects on wet or moist wood and its mechanical properties in the direction perpendicular to the grain (Clorius et al. 2009; Ranta-Manus 1993) are important for the paper industry due to its relevance to mechanical pulping.

Paper industry is aiming at lowering mechanical pulping energy consumption. To this end, it is important to understand the physical and chemical properties of wood used for pulping (Htun and Salmén 1996). Since the 1980s (Young 1985; Frazier and Williams 1982), an effort has been made to find different chemical (Gorski et al. 2011; Johansson et al. 2011; Morris et al. 2000) or mechanical methods and pre-treatments (Viforr and Salmén 2007; Berg 2001; Sabourin 1998) for wood. Wood is refined to fibers either by chemical pulping, i.e., lignin dissolution, or mechanical pulping, i.e., successive compressive and shear loadings. Mechanical pulps are inexpensive and have high yield point, but the energy demand is large. Separating wood fibers using a fatigue pre-treatment can save considerable amounts of energy (Salmi et al. 2012; Engberg et al. 2009; Uhmeier and Salmén 1996b). In particular, a recent study has shown that fatigue treatment softens locally the wood and reduces some of the mechanical properties (Salmi et al. 2009). One of the motivations of the current work is therefore to study the effect of fatigue on the mechanical behavior and characteristics of wood. Later in the present article, experimental evidences of the existence of a softened layer are presented.

Wood is also a heterogeneous and anisotropic (Katz et al. 2008) material due to its micro- and mesoscopic structure (Ando and Onda 1999; Salmén and Burgert 2009); it is a cellular solid (Ando and Onda 1999; Gibson and Ashby 1997) consisting of elongated, submillimeter thick cells which are divided by cell walls consisting of a polymeric composite (Stanzl-Tschegg 2011; Dinwoodie 1975). Above the cell structure, the annual rings correspond to successive layers, in which the size and the density of the cells vary (Stanzl-Tschegg 2011; Dinwoodie 1975) because the wood growth is season-dependent. This material presents two parts: the earlywood and the latewood. Earlywood is the part of wood that grows during spring and presents large cells, unlike latewood. The cells of dense latewood are very thick-walled with very small cell cavities, while those formed first in the season have thin walls and large cell cavities, giving different stiffness inside the wood material. For such reasons, the stress and strain fields are very heterogeneous, and the mechanical response of wood under compression depends strongly on the year rings (Ansell 2011; Ellis and Steiner 2002; Reiterer and Stanzl-Tschegg 2001); this will be further studied in the present article.

The aim of this study is to look at the stress–strain behavior of wood on a centimeter scale while taking into account both the local loading direction and the consequences of a fatigue pre-treatment. Mechanical properties of spruce were considered at microscopic scale and connected with the macroscopic behavior. To this end, the global Young's modulus and the yield point will be compared for fatigued and non-fatigued reference samples.

To study this heterogeneous material, digital image correlation (DIC) was used, which has proven to be a flexible and useful tool for deformation analysis in 2D (Hild and Roux 2006; Kybic and Unser 2003; Pan et al. 2009). The local displacements of a sample under load can be determined with great accuracy and quantified uncertainty (Dupré et al. 2010; Barranger et al. 2010). Therefore, it has been utilized on different anisotropic materials such as composites (Brynk et al. 2012; Carvelli et al. 2010; Fedorov and Berggreen 2010), paper (Miksic et al. 2011a, b; Laurson et al. 2011; Rosti et al. 2010; Mustalahti et al. 2010; Choi et al. 1991), or wood (Xavier et al. 2012; Haldar et al. 2011; Salmén and Burgert 2009; Choi et al. 1991) for instance. Here, the analysis of the local strains gives experimental proof of the existence of a changed—softened—fatigue layer in wood like in Salmi et al. (2011).

The orientation of the annual rings compared to loading direction is examined, as this parameter has proven to be crucial in the mechanical response of wood under compression (Reiterer and Stanzl-Tschegg 2001; Backman and Lindberg 2001; Salmi et al. 2009). It is quantified how the stiffness and the yielding behavior depend on the orientation angle in addition to the fatigue pre-treatment.

The structure of the paper is as follows. The experimental procedures, the exact measurements, and the analysis methods are described in "Methods." In "Results and discussion," the experimental results are presented and discussed. Firstly, the macroscopic mechanical properties, e.g., stiffness, yield stress, and strain, are presented; the influence of the orientation of the annual rings compared to loading direction as well as the differences between fatigued samples and reference ones is highlighted. The next part deals with the local displacements and strain profiles from DIC. The conclusions close the paper in "Conclusion."

Methods

Experimental setup and mechanical procedure

The setup consists of the testing machine which compresses the samples, the camera used for DIC, and the dedicated computers to control and store measurements. Both the machine and the camera are attached to/on a stable rock table to avoid any disturbing moves. Figure 1 shows a photograph of the experiment. An Instron ElectroPulse E1000 testing machine is used with a 1kN Dynacell load cell from the same manufacturer.

At the start of the experiment, an initial preload of 4 N is applied on the wood sample, which is enough to keep the sample from moving, and the camera is then focused. The test procedure is a simple vertical compression at constant displacement speed. The testing machine is operated at a low displacement rate of 0.04 mm/s up to 1 kN, and an experiment lasts around 100 s. When the applied force finally reaches the maximum value, the sample is totally unloaded.

The testing records the synchronized measurements of the load and of the displacement at a frequency of 500 Hz. The accuracy of the load cell is ± 0.5 % of
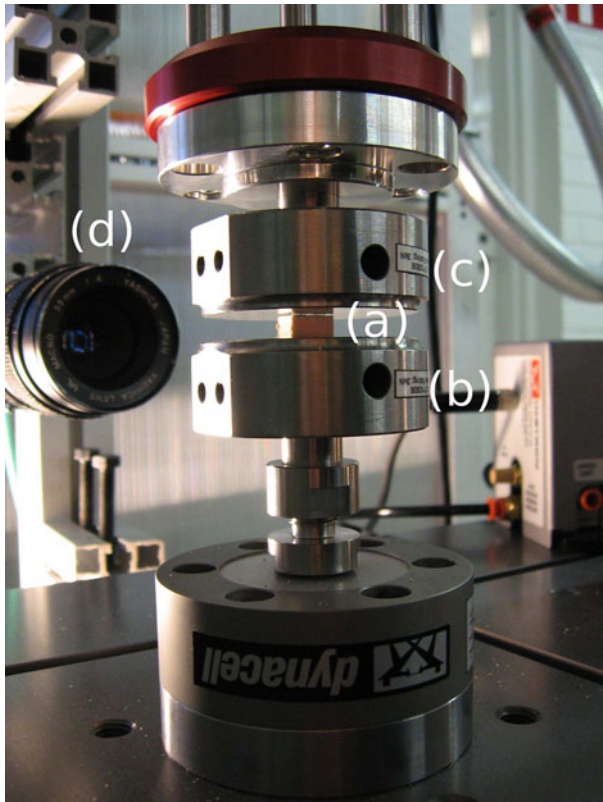
Fig. 1 Experimental setup: **a** the wood sample is put on **b** the fixed *bottom* plate and compressed *vertically* by **c** the moving piston. **d** A camera takes pictures of the sample during compression

the indicated load. The accuracy of the absolute displacement is ±0.3 mm, and the changes in the displacement have an accuracy of ±3 μm.

Sample description and definition of year ring orientation

Two sets of samples from Norway spruce (*Picea Abies*) wood were used as small cubes of around 12 mm edges, cut in planks from the same wood log (Fig. 2a). The difference of the two sample sets was that one set is considered as fresh, whereas the set called fatigued had been pre-treated with high-frequency, high-amplitude cyclic loading. Planks of Norway spruce were cut into $100 \times 100 \times 2$ mm^3 sheets along the plane of the wood annual rings, and the knotless sheets were processed in a loading device. It applies fatigue on one surface at a frequency of 500 Hz during 48 s and with nominal amplitude of 0.75 mm (Salmi et al. 2009, 2012; Engberg et al. 2009). The fatigue pre-treatment affects the material and deforms mostly the earlywood cells as can be seen in the example of figure 6 in Salmi et al. (2012).

The fatigued samples were compared to the reference ones with no treatment. The samples used were precision-machined to the dimensions of 11.6 mm by
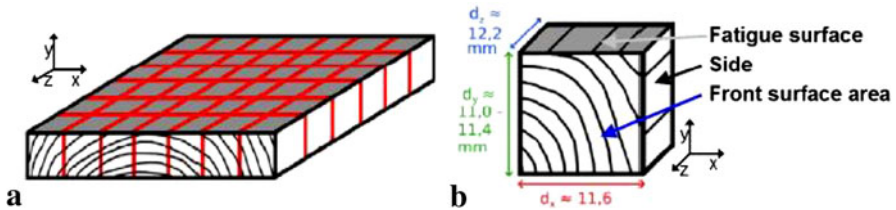
Fig. 2 Details of wood samples—the *grey* surface corresponds to the side on which the fatigue pre-treatment was applied; **a** samples cut from a piece of plank; **b** sample geometry and fatigue application

11.2 mm by 12 ± 0.2 mm, for width, height, and thickness, respectively, with one face being eventually the fatigued surface of the raw fatigued wood plank (Fig. 2b). The fatigued side is left untouched, while all the other sides are machined straight and smooth. All the samples were measured on three sites for each direction, and the average measurement was then used as the size for calculations of stress and strain.

The samples were stored in a freezer at -5 °C and were taken out to melt in a controlled humidifier chamber with relative humidity rh $= 50 \pm 1$ % on the previous day before experiments. Thus, the samples tested were fresh, not (say) oven-dried. This procedure also mimics what the wood goes through during a mechanical pulping process: cutting down in winter, freezing, melting, and pulping.

Initially, the dimensions of a wood timber determine naturally the three directions for cylindrical coordinates: The longitudinal direction corresponds to the growth direction of the wood beam; the radial and tangential directions are defined in the plane of the timber cross section. The radial direction is defined from the center to the outer part of the beam and intersects the annual rings of the wood, while the tangential direction is tangent to the year rings (Fig. 3a).

The orientation angle θ of the annual rings is defined as the angle of the secant of the annual ring, which is the most central one in the sample surface area (Fig. 3b, c). Because of the symmetry properties of the cubic samples of wood, the angle θ is projected to 0°–90° for convenience.

For θ close to 0°, the direction of the applied load is parallel to the year rings and this configuration is defined as tangential loading. For θ increasing up to 90°, the
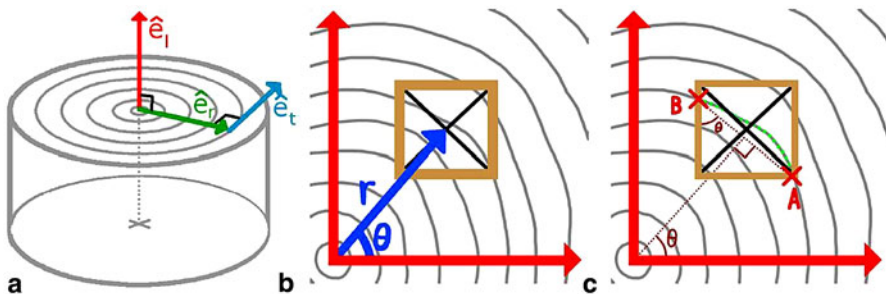

Fig. 3 **a** Natural orthotropic directions of wood; **b** cylindrical coordinates in wood sample; **c** angle θ for the orientation of the annual rings

year rings get more and more perpendicular to the vertical axial load and this corresponds to a radial loading.

Data acquisition and analysis for macroscopic properties

The values of strain and stress are defined here positive for compression. The usual stress–strain curve is nonlinear and displays three parts of varying length: an elastic regime at the beginning, then a plastic plateau (crushing/buckling), and finally a sharp increase before the end. The Young's modulus of elasticity E is defined as the steepest slope (dashed line in Fig. 4) at a point (ε_E, σ_E) of the first elastic part:

$$E = \max_{\varepsilon}\left(\frac{d\sigma}{d\varepsilon}\right).$$

The yield point (ε_Y, σ_Y) is defined as the point where the stress differs by 10 % from the perfectly elastic case (Fig. 4). The zero strain ε_0 is defined as the point where the maximum slope crosses $\sigma = 0$.

The definitions above are similar to the output from a standard tensile-testing machine. The definitions are important as the shape of the stress–strain curve changes with fatigue process as well as with the annual ring orientation.

In order to quantify the behavior in the plateau-like part of the stress–strain curve, the curves in this second phase were divided into two parts and a linear regression was performed for each part independently (i.e., not forcing the two linear parts to form a continuous curve).

Digital image correlation technique for local deformation and damage

For the image registration technique (Hild and Roux 2006; Kybic and Unser 2003), a 1-megapixel digital camera records the experiment to a sequence of pictures. The camera captures ten frames per second at an image resolution of 1,024 by 768 pixels. One millimeter corresponds to approximately 70 pixels. The images are

Fig. 4 Definition of stiffness, yield point, and zero deformation on the stress–strain curve
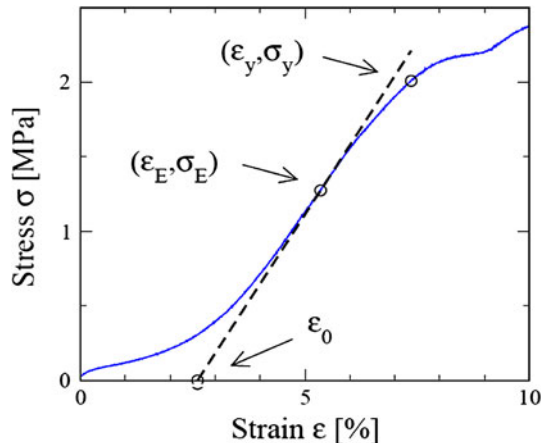
processed with the algorithm described in Mustalahti et al. (2010). The output of the algorithm is a matrix of the local displacement vectors from which the local strain tensor is calculated.

This method has limitations on how far in an experiment it can be used. As the sample is more and more deformed, comparing pictures to the first one gets harder and harder, and at some point, the DIC software fails to find the correct deformation. The limit seems to be around 50 s, corresponding to a strain of around 0.15 (i.e. 15 %), in the present experiments. For most samples, the yield point is reached before this.

Results and discussion

Effects of orientation of annual rings and fatigue treatment at macroscopic scale

The typical stress–strain curves are shown in Fig. 5 for a representative set of reference and fatigued samples: The usual three stages of the compression of a cellular solid (Gibson and Ashby 1997) are visible. The first elastic part corresponds to the compression of the cell walls and lasts until reaching a strain value of around 0.05–0.06 for a stress between 2 and 4.5 MPa. Then, the plateau part, coming from cell wall buckling, starts. In closed cell foams like in wood, the gas pressure increase at the cell lumens is known to also cause a stress increase during the buckling phase. After elimination of all the voids, densification starts (Gibson and Ashby 1997) and a sharper increase of the stress within a short strain appears at the end of a test before unloading. The vertical strain ε_{yy} reaches 35–55 % for a stress of circa 7 MPa.

A combined effect of the fatigue pre-treatment and the orientation angle of the wood annual rings is observed on the global stress–strain curves. In general, the stress–strain curves are much smoother and less steep on the first elastic part for the samples which have undergone fatigue pre-treatment, whereas the reference samples display a steep beginning and nearly horizontal or even negative slope plateaus on the stress–strain curves. The plateau parts in the fatigued samples are

Fig. 5 Macroscopic stress–strain curves for compression tests on reference (*continuous lines*) or fatigued samples (*dotted lines*) for different orientations of the year rings (*colors*)
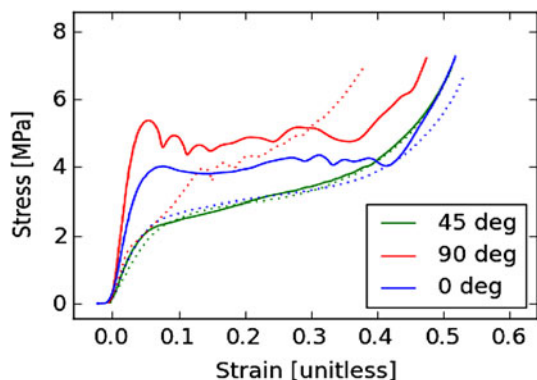
smoother and steeper. For angles θ close to 45°, the stress–strain curves are smooth and only a slight difference between the fatigued samples and the reference ones appears.

Figure 6 shows the Young's modulus in both cases of fatigued and reference samples: It presents a minimum value in samples with slanted year rings. In the reference samples, the modulus presents a minimum of $E = 47$ MPa for $\theta = 45°$, and the minimum value is $E = 43$ MPa for $\theta = 50°$ in fatigued samples. When $\theta < 45°$, the Young's moduli in reference and fatigued samples are very similar, though the latter ones have slightly lower values in general. In radial loading (for $\theta = 90°$), the Young's modulus of a fatigued sample is almost four times smaller than in a reference sample. This difference gets smaller as the orientation angle decreases to $\theta = 45°$. The corresponding literature value for fresh wood under radial loading is $E = 350$ MPa (Koponen et al. 2005; Bodig and Goodman 1973), very close to the measurement results of the present study, around 340 MPa.

The yield stress displayed in Fig. 7 shows the same typical features as the Young's modulus for reference samples: a minimal value around 1 MPa for θ close to 45° and higher values in case of radial and tangential compression. For $\theta = 90°$, the reference samples have a yield stress of 1.5–4 MPa, which is clearly higher than for fatigued samples, where $\sigma_Y < 2.5$ MPa. In case of $\theta < 60°$, the yield stresses of the fatigued and reference samples are almost the same, although σ_Y for fatigued wood seems slightly higher than in non-fatigued one, and σ_Y decreases from circa 5 to 1 MPa for θ increasing from 0° to 45° in both sets of samples. The yielding behavior of late wood is presumably not changed in fatigue treatment.

Figure 8 shows that the yield strain ε_Y seems generally larger in fatigued samples for θ between 20° and 60° than in reference samples, but the two sample sets present very close yield strains otherwise. Globally, the range of values for ε_Y in reference samples is wider than in fatigued samples (Table 1). Multiplying the yield strain by the Young's modulus gives an evaluation of the yield stress higher than the measured one by a factor of 1.42 ± 0.14 for fatigued samples and 1.44 ± 0.24 for
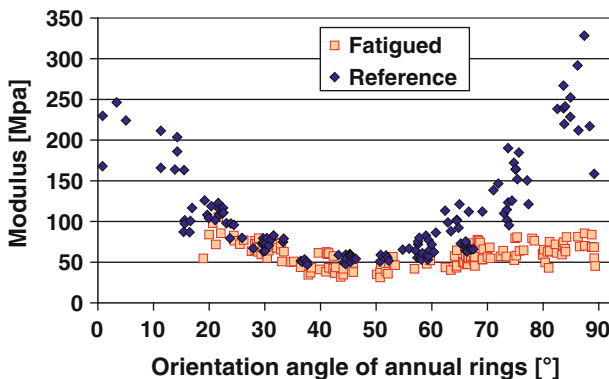

Fig. 6 Young's modulus for compression tests on reference (*light red squares*) and fatigue samples (*dark blue diamonds*) for different orientations
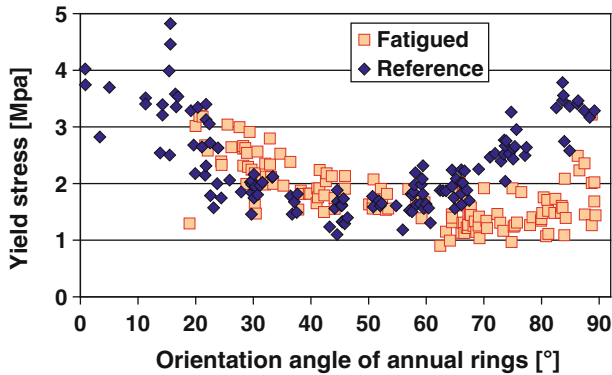
Fig. 7 Yield stress of reference (*light red squares*) and fatigue samples (*dark blue diamonds*)
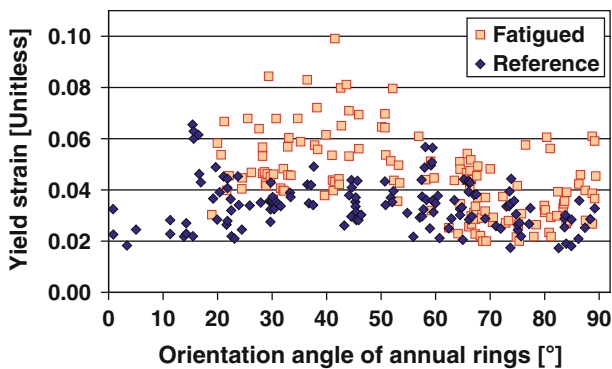

Fig. 8 Yield strain of reference (*light red squares*) and fatigue samples (*dark blue diamonds*)

reference samples, but the so-calculated yield stress presents a similar curve shape as a function of the orientation angle.

Finally, the slopes of both plateau parts depend strongly on the orientations of the annual rings, and a clear effect from the fatigue treatment appears in particular for the radially loaded samples (Figs. 9, 10): The slopes of the plateau parts are higher for fatigued samples than for non-fatigued ones. In particular, the first part of the plateau displays a more visible effect from fatigue than the second part (Figs. 9, 10). The reference samples present irregularities on the curves in the case of radial loading, and to a less extent for the tangential loading case. The bumps on the plateau (Fig. 5) are due to the sudden collapse of the weakest layers of the annual rings. In the case of tangentially loaded samples, this effect is less important, and small local shear of the wood can be observed on the weakest part too. In fatigued samples, the sudden collapses do not occur because the weakest layers have already been deformed during the fatigue treatment. Thus, the stress–strain curves are smoother but also the plateau is less flat but steeper. The samples with an orientation of the annual rings at around 45° compared to the load direction encounter larger shear.

Table 1 Summary of the values of the mechanical parameters for reference and fatigued samples; yield strain are without unit, and other values are in MPa

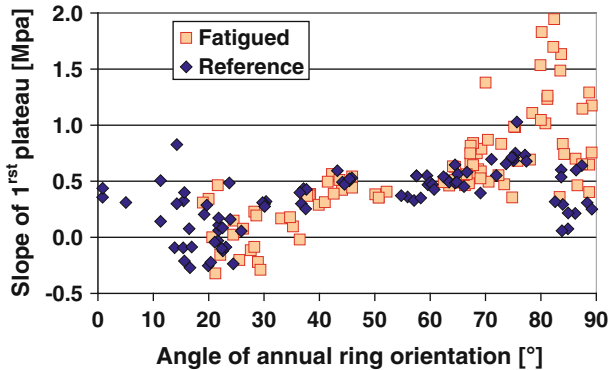|	Reference	Fatigue
Young's modulus	47 to 328	43 to 105
Yield strain	0.017 to 0.066	0.020 to 0.099
Yield stress	0.9 to 3.2	1.1 to 4.8
Plateau slope 1	−0.32 to 1.95	−0.27 to 1.03
Plateau slope 2	−0.37 to 1.22	−0.31 to 0.97

Fig. 9 Slope of the first half of the plateau of reference (*light red squares*) and fatigue samples (*dark blue diamonds*)
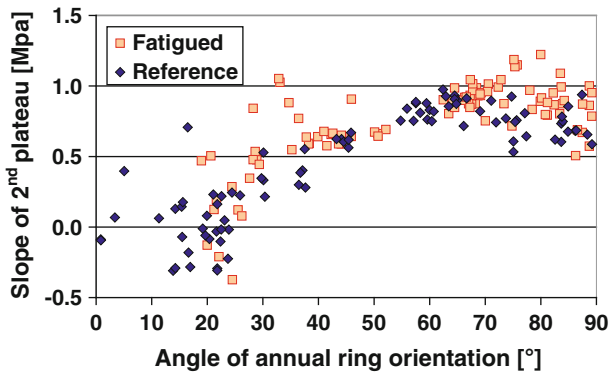

Fig. 10 Slope of the second half of the plateau of reference (*light red squares*) and fatigue samples (*dark blue diamonds*)

These observations mean that the fatigue treatment changes globally the mechanical response of the wood: It decreases the wood stiffness in the elastic part and lowers the yield stress, but the plateau part in reference samples is longer and less steep than in fatigued samples.

Comparison with earlier results

First, it should be noticed that the values for the modulus measured here are lower than in Bodig and Goodman (1973) where the modulus of Norway spruce was studied by ultrasound and found to be 1 ± 0.15 GPa and 0.35 ± 0.04 GPa in the radial and tangential directions, respectively. This comes probably from the difference between the two methods and the role of wood viscoelasticity in ultrasound. It is rather interesting to note that, in the present experiments in which the loading is always perpendicular to the longitudinal direction (see Fig. 3a), the obtained values for modulus are much lower than in the case where the load is applied longitudinally (Dahl and Malo 2009), where the measured modulus of elasticity is spread from around 4 to 24 GPa. The values for the modulus of elasticity are less spread than those observed in Garab et al. (2010) for different orientation angles in spruce—only from 95 to 211 MPa—even if they are still rather close to each others.

The literature on the wood mechanics and annual ring orientations (Ansell 2011; Ellis and Steiner 2002; Reiterer and Stanzl-Tschegg 2001) mainly focuses on orientations which are between the radial and the longitudinal directions of wood. Ellis and Steiner (2002) observed that for five different species of wood under simple compression, the Young's modulus and the stress level are higher in longitudinally loaded samples than for transversely loaded ones. In the present experiments, it was shown that the Young's modulus is higher in radial-loaded samples than in tangential-loaded ones. A result, similar to these experiments on non-fatigued wood, is displayed in figure 6a in Ansell (2011) resulting from Backman and Lindberg (2001) and in table 1 in Salmi et al. (2009). The experiments on Scots pine (Backman and Lindberg 2001) clearly show the value of tangential Young's modulus E_T to be always lower than the radial one E_R. In spruce (Garab et al. 2010), this observation is still true and the same trend for the Young's modulus is observed: A minimum appears for an angle of 45° in Garab et al. (2010).

In Reiterer and Stanzl-Tschegg (2001), the changes in Young's modulus, Poisson's ratio, and crushing strength were compared for different orientations of the annual rings with respect to the radial and longitudinal direction. This study is interesting to compare with the results of the present study, because the deformations in the wood samples are very similar, in particular in radial loading. In the experiments of the present work, collapses inside different annual rings of the wood for radially loaded samples were observed, similar to figure 13b in Reiterer and Stanzl-Tschegg (2001). This phenomenon of local collapse will be discussed further in the next section. In addition, accordion-like deformations, similar to figure 12b in Reiterer and Stanzl-Tschegg (2001), are visible in the samples here for θ close to 70°–80°. The same authors present, in figure 8 of this article, the local shear deformation in wood; the same kind of shear bands deformation was observed here in the samples with $\theta \approx 45°$, but without any delamination. It is thought that this shear effect is responsible for the low values of Young's modulus and yield stress in these samples.

In addition to the effect of annual ring orientation discussed previously, the fatigue treatment clearly affects the mechanical behavior of wood. Firstly, it

diminishes the Young's modulus of the wood samples, as observed by Salmi et al. (2012). The authors used an ultrasonic method to measure the stiffness of Norwegian spruce in case of fatigue loading at high strain rates. The stiffness of the dry wood was observed to decrease with the number of loading cycles. Similar results were found by Engberg et al. (2009) where an encapsulated Split-Hopkinson method was used to study Norway spruce compressed at high strain rate. In figure 3 by Engberg et al., the stress–strain curves for tests at room temperature show clearly that the Young's modulus becomes lower if the fatigue treatment is more intensive. Moreover, the authors also discussed an effect of fatigue on the plateau part, similar to the results of the present study in Fig. 9: the plateau part of the stress–strain curve is steeper for more fatigued samples.

Deformation at local scale inside the year rings

Local displacements were studied using DIC. Figures 11 and 12 depict snapshots of displacements and strains along the compression axis, respectively. These two graphs actually show how the fatigue effect is localized to the surface of the sample.

Figure 11 shows the displacement profiles for four representative samples. The displacement profile is the y-component of the displacement along the center axis, taken at the center of the sample width, at time $t = 15$ s. This is at, or just before, the yield point (see Fig. 5 for comparison). Figure 12 depicts the vertical strain corresponding to the vertical displacement in radially loaded samples from Fig. 11. Both data are displayed as a function of y, the height (or the distance) from the fatigued surface, or from the normal raw surface in reference samples. In Fig. 12, a steep slope near the edge is visible at $y = 0$ for the strain in the reference samples, while the slope is not so steep in the fatigue ones. This Figure emphasizes that the difference between earlywood layers becomes smaller in fatigued samples.

The reason for such displacement or strain behavior near the surface has two origins. Firstly, the fatigue treatment affects the surface layer. Secondly, the coupling between the sample and the compression device is not ideal. The fatigue treatment softens a surface layer of 2 mm. This phenomenon is perhaps more

Fig. 11 Displacement profile as a function of height along axis of compression, at time $t = 15$ s; *red curves* correspond to radially loaded samples, and the tangentially loaded samples are depicted in *blue*
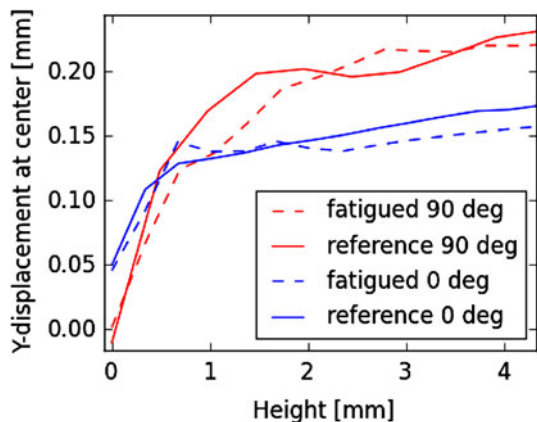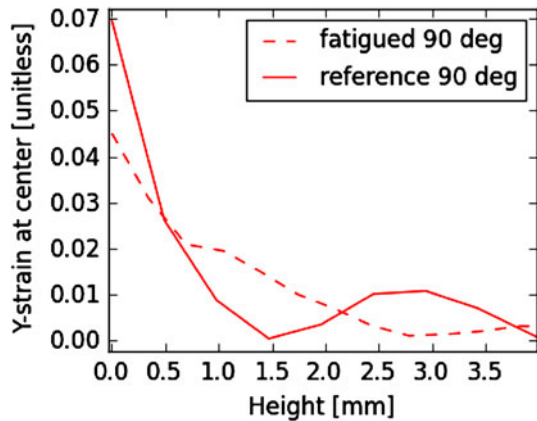
Fig. 12 Strain profile as a
function of height along axis of
compression for, fatigued and
reference, radially loaded
samples ($\theta \approx 90°$) at time
$t = 15$ s

clearly seen in Fig. 12, where the strain at a distance of 2 mm from the surface
equals the typical strain of the sample. From the strain profiles, it can also be
concluded that the difference between earlywood layers is larger in the reference
samples than in the fatigued case. This is seen most clearly in the radial loading case
($\theta \approx 90°$; the solid red line in Fig. 11), where the strain is concentrated in a few
annual rings only.

In the 45° case, the strain concentration is due to shearing of the wood, as in the
90° case, the cause is annual ring collapse. One can compare the softening effect to
the results in Fig. 6 where the modulus is lower for the fatigued case, i.e., the
material is softer. In addition to softening, the data for the first 0.5 mm are affected
by the surface roughness. The reference samples have rough surfaces that lower the
modulus. The fatigue treatment makes the surfaces smooth. Another phenomenon
affecting the top layer is the Poisson effect. The interface between the piston and the
wood has high friction, and the wood cannot expand. This creates shear stresses.

In the radial case ($\theta \approx 90°$ and annual rings perpendicular to load) of the pre-
fatigued wood, the incline is expected to result from nonuniform stiffness. The cells
that are fatigued the most buckle and collapse at low stress and stiffer, and stiffer
cells pass gradually the yield point. In the other cases when the load is not anymore
perpendicular to the annual rings, the stiff latewood, which seems not affected by
fatigue treatment, probably carries the stress in fatigued and in reference samples,
and the displacement (blue curves Fig. 11) is therefore smaller than in radial
loading. The latewood, being much stiffer, remains without deformation in both
fatigued and reference samples. In fresh wood, the deformation in earlywood is
much larger than in the pre-fatigued specimens.

The different densities inside annual rings are shown in figure 11 in Reiterer and
Stanzl-Tschegg (2001), and the differences in the wood cell sizes are also visible
here in Fig. 2 of this study here. The largest cells in the latewood are more deformed
than the small cells of latewood in case of reference samples. The soft earlywood
layers are deformed more in compression, as shown by Saari et al. (2009) in Norway
spruce wood. Much larger unevenly distributed deformations appear in soft
earlywood than in latewood where the strain was always very small, even after a

high fatigue treatment. The local differences in strain were attributed to the weakness of thin walled earlywood cells. Moreover, the difference in stiffness of latewood and earlywood and the fact that the fatigue treatment affects almost only the soft earlywood can explain the different stress–strain curve shapes observed in the part of the present article about "Effects of orientation of annual rings and fatigue treatment at macroscopic scale."

In addition, the creation of a softener layer from fatigue treatment is clearly observed and quantified in the results here; it is furthermore supported in the literature. In Salmi et al. (2012), the authors used an ultrasonic method to obtain the depth profiles of Young's modulus inside wood after grinding, and they observed a distinct layer where the elastic modulus is lower than that of the intact part in the ground wood. In Lucander and Björkqvist (2005), the authors predict via simulations that the elastic compression inside the wood reaches a depth of around 0.1–0.2 mm, smaller than the fatigue layer measured in the experiments of the present study. However, the experiments realized in Salmi et al. (2011) show that the use of a wave-shaped grindstone to apply a grinding treatment on wood creates a layer of around 0.5–1.5 mm in which the stiffness modulus is decreased by 80 % compared to the modulus in non-ground wood. Such a reduction is comparable to the results here for the modulus, in particular for the orientation angles of the annual rings close to 45°, where the results in fatigued and reference samples are the closest.

Conclusion

Using DIC and macroscopic stress–strain measurements, experiments on samples of Norway spruce wood with different orientations of the annual rings relative to the load direction were examined. The effect, at different scales, of a fatigue treatment mimicking mechanical pulping was compared. The results obtained from the axial compression experiments exhibit the nonlinear mechanical behavior of the wood with a clear effect of the fatigue.

The results confirm the strong effect of the direction of the annual rings in the wood under compression, in directions perpendicular to the grain. Moreover, the importance of the fatigue treatment on the mechanical properties of wood in different cases of loading from tangential to radial direction was quantified.

The fatigue treatment lowers the elastic modulus and the yield stress, and the effect is maximal if the loading is done in radial direction. An increase in yield strain somewhat compensates making the decrease in yield stress less pronounced than the decrease in stiffness. In addition, the fatigue effect is in particular concentrated on the surface of the sample, in a softened layer of a few millimeters. This phenomenon is due to the dynamic nature of the fatigue application.

It is concluded that the mechanical energy that is generated by the fatigue treatment is absorbed close to the adjacent surface of the sample. This alters the cell structure of the wood and modifies the mechanical properties. It would be of interest to extend the current results and apply high resolution DIC method to a variety of cases with different—higher—temperatures and wood water contents. The

motivation for such research comes both from the relevance for applications to mechanical pulping and from interest in the softening effects of water and higher temperatures.

References

Ando K, Onda H (1999) Mechanism for deformation of wood as a honeycomb structure. J Wood Sci 45(3):250–253

Ansell M (2011) Wood—a 45th anniversary review of JMS papers. Part 1: the wood cell wall and mechanical properties. J Mater Sci 46(23):7357–7368

Armstrong L, Kingston R (1960) Effect of moisture changes on creep in wood. Nature 185:862–863

Backman A, Lindberg K (2001) Differences in wood material responses for radial and tangential direction as measured by dynamic mechanical thermal analysis. J Mater Sci 36(15):3777–3783

Barranger Y, Doumalin P, Dupré J-C, Germaneau A (2010) Digital image correlation accuracy: influence of kind of speckle and recording setup, EPJ Web of Conferences, vol 6, Article number 31002, for ICEM14

Berg J-E (2001) Effect of impact velocity on the fracture of wood as related to the mechanical pulping process. Wood Sci Technol 35(4):343–351

Bodig J, Goodman J (1973) Prediction of elastic parameters for wood. Wood Sci 5(4):249–264

Brynk T, Molak R, Janiszewska M, Pakiela Z (2012) Digital image correlation measurements as a tool of composites deformation. Comput Mater Sci 64:221–224

Carvelli V, Tomaselli V, Lomov S, Verpoest I, Witzel V, Broucke B (2010) Fatigue and post-fatigue tensile behavior of non-crimp stitched and unstitched carbon/epoxy composites. Compos Sci Technol 70(15):2216–2224

Choi B, Thorpe JL, Hanna RB (1991) Image analysis to measure strain in wood and paper. Wood Sci Technol 25(4):251–262

Clorius C, Pedersen M, Hoffmeyer P, Damkilde L (2009) An experimentally validated fatigue model for wood subjected to tension perpendicular to the grain. Wood Sci Technol 43(3–4):343–357

Dahl K, Malo K (2009) Planar strain measurements on wood specimens. Exp Mech 49:575–586

Dinwoodie J (1975) Timber—a review of the structure—mechanical property relationship. J Microsc 104(1):3–32

Dupré J-C, Bornert M, Robert L, Wattrisse B (2010) Digital image correlation: displacement accuracy estimation, EPJ web of conferences 6, 31006, for ICEM14

Ellis S, Steiner P (2002) The behaviour of five wood species in compression. IAWA J 23(2):201–211

Engberg B, Salminen L, Salmi A, Björkqvist T, Lucander M (2009) On the importance of fatigue for the rheological properties of wood. In: Proceedings—international mechanical pulping conference, IMPC 2009, pp 239-244 (IMPC 2009; Code79937)

Fedorov V, Berggreen C (2010) Multi-axial load application and DIC measurement of advanced composite beam deformation behavior EPJ Web of Conference 6, Article number 16006

Findley W, Lai J, Onaran K (1989) Creep and relaxation of nonlinear viscoelastic materials. Dover Publications, New York, pp 239–248

Frazier WC, Williams GJ (1982) Reduction of specific energy in mechanical pulping by axial precompression of wood. Pulp Pap Can 83(6):87–92

Garab J, Keunecke D, Hering S, Szalai J, Niemz P (2010) Measurement of standard and off-axis elastic moduli and Poisson's ratios of spruce and yew wood in the transverse plane. Wood Sci Technol 44(3):451–464

Gibson LJ, Ashby MF (1997) Cellular solids. Cambridge University Press, Cambridge

Gorski D, Mörseburg K, Axelsson P, Engstrand P (2011) Peroxide-based ATMP refining of spruce: energy efficiency, fibre properties and pulp quality. Nord Pulp Pap Res J 26(1):47–63

Haldar SI, Gheewala N, Grande-Allen K, Sutton M, Bruck H (2011) Multiscale mechanical characterization of palmetto wood using digital image correlation to develop a template for biologically-inspired polymer composites. Exp Mech 51(4):575–589

Hanhijärvi A, Hunt D (1998) Experimental indication of interaction between viscoelastic and mechano-sorptive creep. Wood Sci Technol 32(1):57–70

Hild F, Roux S (2006) Digital image correlation: from displacement measurement to identification of elastic properties—a review. Strain 42:69–80

Htun M, Salmén L (1996) The importance of understanding the physical and chemical properties of wood to achieve energy efficiency in mechanical pulping. Wochenblatt für Papierfabrikation 124(6):232–235

Jäger A, Bader Th, Hofstetter K, Eberhardsteiner J (2011) The relation between indentation modulus, microfibril angle and elastic properties of wood cell walls. Compos A Appl Sci Manuf 42(6):677–685

Johansson L, Hill J, Gorski D, Axelsson P (2011) Improvement of energy efficiency in TMP refining by selective wood disintegration and targeted application of chemicals. Nord Pulp Pap Res J 26(1):31–46

Kärenlampi P, Tynjälä P, Ström P (2003) Effect of temperature and compression on the mechanical behavior of steam-treated wood. J Wood Sci 49(4):298–304

Katz L, Spencer P, Wang Y, Misra A, Marangos O, Friis L (2008) On the anisotropic elastic properties of woods. J Mater Sci 43:139–145

Keckes J, Burgert I, Frühmann K, Müller M, Kölln K, Hamilton M, Burghammer M, Roth S, Stanzl-Tschegg S, Fratzl P (2003) Cell wall recovery after irreversible deformation of wood. Nat Mater 2:810–813

Koponen T, Karppinen T, Hæggstöm E, Saranpää P, Serimaa R (2005) The stiffness modulus in Norway Spruce as a function of year ring. Holzforschung 59(4):452–455

Kybic J, Unser M (2003) Fast parametric elastic image registration. IEEE Trans Image Process 12(11):1427–1442

Laurson L, Rosti J, Koivisto J, Miksic A, Alava MJ (2011) Spatial fluctuations in transient creep deformation. J Stat Mech: Theory Exp P07002:1–27

Lucander M, Björkqvist T (2005) New approach on the fundamental mechanisms in wood grinding, International mechanical pulping conference, Oslo, Norway, 7–9 June 2005. Proceedings, pp 149–155

Miksic A, Koivisto J, Alava MJ (2011a) Statistical properties of low cycle fatigue in paper. J Stat Mech: Theory Exp P05002:1–26

Miksic A, Koivisto J, Rosti J, Alava M (2011b) Strain fluctuations from DIC technique applied on paper, ICM11, Lake Como Italy, 5–9 June 2011. Procedia Eng 10:2678–2683

Morris D, Steward F, Gilmore C (2000) Comparative analysis of the consumption of energy of two wood pulping processes. Energy Convers Manage 41(14):1557–1568

Murata K, Masuda M (2001) Observation of the swelling behavior of coniferous cells using a confocal scanning laser microscope and a digital image correlation method. Mater Sci Res Int 7(3):200–205

Mustalahti M, Rosti J, Koivisto J, Alava M (2010) Relaxation of creep strain in paper. J Stat Mech Theory Exp P07019:1–19

Navi P, Stanzl-Tschegg S (2009) Micro-mechanics of creep and relaxation of wood. A review. Holzforschung 63:186–195

Ozyhar T, Hering S, Niemz P (2012) Moisture-dependent elastic and strength anisotropy of European beech wood in tension. J Mater Sci 47(7):1–10

Pan B, Qian K, Xie H, Asundi A (2009) Two-dimensional digital image correlation for in-plane displacement and strain measurement: a review. Meas Sci Technol 20(6):Number 062001, 1–17

Ranta-Manus A (1993) Rheological behaviour of wood in directions perpendicular to the grain. Mater Struct 26(6):362–369

Reiterer A, Stanzl-Tschegg S (2001) Compressive behaviour of softwood under uniaxial loading at different orientations to the grains. Mech Mater 33:705–715

Rosti J, Koivisto J, Laurson L, Alava MJ (2010) Fluctuations and scaling in creep deformation. Phys Rev Lett 105:100601

Saari V, Björkqvist T, Engberg B, Saarenrinne P (2009) Strain distribution in annual rings under compression by high speed photography. In: Proceedings—2009 international mechanical pulping conference, IMPC 2009, pp 245–251

Sabourin M (1998) Evaluation of a compressive pretreatment process on TMP properties and energy requirements. Annual meeting—technical section, Canadian Pulp and Paper Association, Preprints, Pt B, pp B41–B50

Salmén L, Burgert I (2009) Cell wall features with regard to mechanical performance. A review. COST action E35 2004–2008: wood machining—micromechanics and fracture. Holzforschung 63(2): 121–129

Salmi A, Salminen L, Hæggström E (2009) Quantifying fatigue generated in high strain rate cyclic loading of Norway spruce. J Appl Phys 106(104905):1–5

Salmi A, Saharinen E, Hæggström E (2011) Layer-like fatigue is induced during mechanical pulping. Cellulose 18(6):1423–1432

Salmi A, Salminen L, Lucander M, Hæggström E (2012) Significance of fatigue for mechanical defibration. Cellulose 19(2):575–579

Schniewind A, Barrett J (1972) Wood as a linear orthotropic viscoelastic material. Wood Sci Technol 6:43–57

Stanzl-Tschegg S (2011) Wood as bio-inspiring material. Mater Sci Eng, C 31:1174–1183

Uhmeier A, Salmen L (1996a) Influence of strain rate and temperature on the radial compression behavior of wet spruce. J Eng Mater Technol Trans ASME 118(3):289–294

Uhmeier A, Salmen L (1996b) Repeated large radial compression of heated spruce. Nord Pulp Pap Res J 11(3):171–176

Viforr S, Salmén L (2007) Shear/compression treatment of wood material—a way of reducing energy demand in TMP processes. International mechanical pulping conference 2007, TAPPI, pp 1038–1044

Wildehammar S (2004) Stress-strain relationships for spruce wood: influence of strain rate, moisture content and loading direction. Exp Mech 44(1):44–48

Xavier A, De Jesus J, Morais A, Pinto J (2012) Stereovision measurements on evaluating the modulus of elasticity of wood by compression tests parallel to the grain. Constr Build Mater 26(1):207–215

Young R (1985) Organic acid pulping of wood reduces chemical costs and energy requirements. Pap Trade J 169(11):50–51